



# Simultaneous study of anionic polymerization of $\epsilon$ -caprolactam and crystallization of polyamide 6 in an isothermal process by in situ WAXS

Mamiko Narita<sup>1</sup> · Hiroaki Yoneyama<sup>1</sup> · Takuro Matsunaga<sup>1</sup> · Masashi Harada<sup>1</sup>

Received: 8 July 2019 / Revised: 9 August 2019 / Accepted: 14 August 2019 / Published online: 9 September 2019  
© The Society of Polymer Science, Japan 2019

## Abstract

We directly observed the polymerization and crystallization of polyamide 6 (PA6) via anionic polymerization with a combination of in situ wide-angle X-ray scattering (WAXS), temperature measurements, and real-time visualization. In situ WAXS discriminated polymerization and the crystallization of PA6. The peak temperatures produced by exothermic polymerization and crystallization were identified during the temperature measurements. Visual observations were consistent with the WAXS spectral changes. The WAXS results indicated that the molding process consisted of three stages: (1) polymerization induction, (2) polymerization, and (3) crystallization. We compared the polymerization rate, crystallization rate, and crystallinity at each molding temperature. Both polymerization and crystallization were slow at temperatures below 127 °C. Polymerization was fast at temperatures exceeding 166 °C, but PA6 was gelled, and the crystallization rate and crystallinity were low. In contrast, polymerization was fast at 139, 148, and 155 °C, and crystallization was faster at 148 and 155 °C than at 139 °C. Therefore, the total molding time of PA6 was shorter at 148 and 155 °C than at other temperatures. The crystallinity of PA6 decreased with increasing temperature due to increasing molecular weights. We concluded that molding temperatures between 148 and 155 °C were suitable for providing PA6 with high productivities and good properties.

## Introduction

The anionic polymerization of  $\epsilon$ -caprolactam (CL) yields polyamide 6 (PA6), known as monomer-cast PA6 (MCPA6). PA6 produced via anionic polymerization has useful properties that differ from those of PA6 obtained from hydrolytic processes (hPA6). These properties include a high modulus, a low tendency to absorb water due to increased molecular weight and good crystallinity [1]. Anionic polymerization of CL is a bulk process that requires a monomer, an initiator, an activator, and molding at a temperature several degrees below the melting point of

PA6. Because the viscosity of CL solutions is low [2], MCPA6 has received a great deal of attention for use in continuous or long fiber-reinforced thermoplastics (FRTPs). FRTPs require not only high performance but also high productivity. The high molecular weight and crystallinity of MCPA6 make it more suitable for use in FRTPs than hPA6. MCPA6 molding takes several minutes; therefore, it is a slower process than injection molding of hPA6. Reducing the time required for molding would make MCPA6 more attractive for use in FRTPs. However, anionic polymerization of CL and PA6 crystallization both take place during the molding step. Reducing the duration of the MCPA6 molding step thus requires increases in the polymerization and crystallization rates. The polymerization rate, the crystallization rate, and the relationship between the two have been investigated with differential scanning calorimetry (DSC) [3, 4], infrared spectroscopy [4], calorimetry [5–7], and microscopy [4]. Sibal et al. [5] suggested that the kinetics of sodium-catalyzed anionic CL polymerization make this reaction suitable for injection molding. They monitored temperature changes during the reaction under adiabatic conditions. They found that at low initial

**Supplementary information** The online version of this article (<https://doi.org/10.1038/s41428-019-0262-8>) contains supplementary material, which is available to authorized users.

✉ Mamiko Narita  
naritam@mosk.tytlabs.co.jp

<sup>1</sup> Toyota Central Research & Development Laboratories, Inc., 41-1 Yokomichi, Nagakute, Aichi 480-1192, Japan

temperatures of  $\leq 130$  °C, crystallization occurred during the polymerization step and that crystallization was delayed when the initial temperature was 160 °C or higher. Davé et al. [6] studied the polymerization and crystallization kinetics of a carbamoyl-type CL/magnesium bromide caprolactamate system in an adiabatic reactor. They monitored the temperature during the molding step and calculated the kinetics parameters. Rijswijk et al. [8, 9] studied polymerization conditions for the manufacture of large thermoplastic composites via a vacuum infusion process. They showed that the polymerization time could be reduced when a combination of carbamoyl-type CL and sodium caprolactamate was used. They also determined the polymerization temperature at which the optimum mechanical properties were attained. They attained the highest reaction rate and density at temperatures between 140 and 150 °C, which yielded optimal MCPA6 properties.

These researchers employed indirect methods to observe polymerization and crystallization under conditions that differed from typical isothermal FRTP molding conditions. Direct observation of the polymerization and crystallization processes under isothermal conditions would be useful for optimizing the molding of high-performance MCPA6. We thus propose a method for the direct observation of polymerization and crystallization under conditions similar to those typically used for molding FRTPs. Time-resolved wide-angle X-ray scattering (WAXS) enabled direct observation of polymerization and crystallization in real time. Polymerization reduced the distance between molecules, while crystallization created a periodic structure. The

progression of these processes was indicated by changes in the WAXS spectra. The changes were observed in different regions of the spectra; thus, the polymerization and crystallization processes could be distinguished and monitored in real time. Herein, we report the direct observation of the MCPA6 polymerization and crystallization processes using a combination of in situ WAXS, temperature measurements and visual inspection in real time. The carbamoyl-type CL/sodium caprolactamate polymerization system was selected because it is halogen-free and reduces the time required for molding [1, 10]. Reaction temperature measurements, visual observation, and in situ WAXS were performed simultaneously. The relationships between the polymerization and crystallization rates and temperature were investigated, and we determined the optimal temperature for efficient production of MCPA6.

## Materials and methods

### Setup for simultaneous measurements

Simultaneous WAXS analysis, temperature measurements and image collection were performed with the experimental setup shown in Fig. 1. The setup consisted of a heating unit and a sample unit on a supportive base, a WAXS detector, a web camera, and a data logger (Fig. 1a). The heating unit had an inlet for incident X-rays, an inlet for connection to the observation vessel, and a window facing the detector for the detection of scattered X-rays. The WAXS detector and

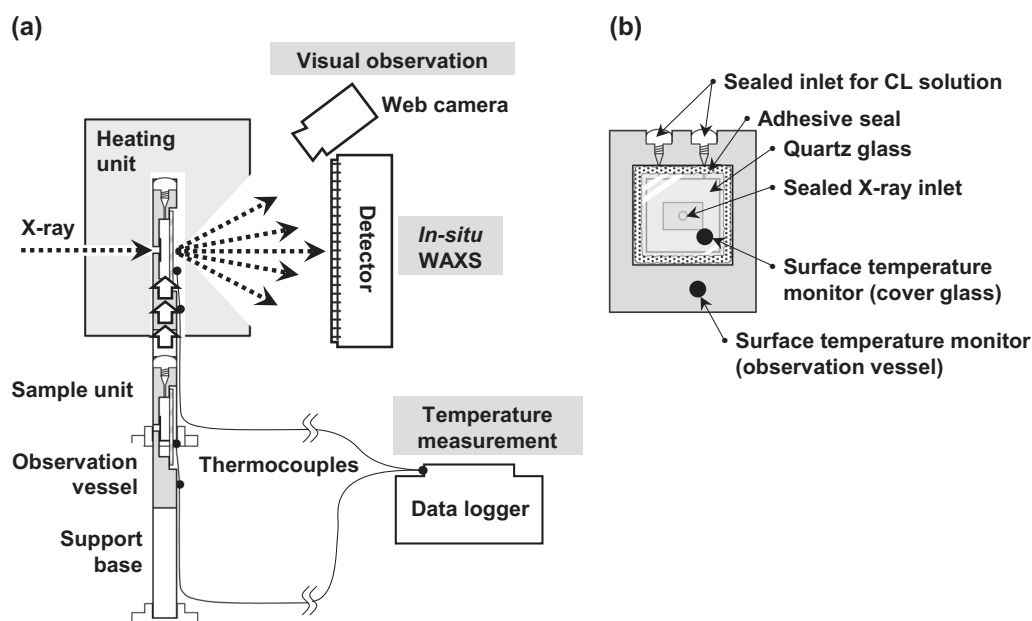


**Fig. 1** Schematic illustration of the experimental apparatus. **a** Setup for simultaneous observation of MCPA6 polymerization and crystallization. **b** Diagram of the observation vessel

web camera were placed on the same side of the apparatus. The incident X-ray inlet was sealed with polyimide tape, and a quartz glass observation window was sealed with a heat-resistant adhesive (Fig. 1b). Two thermocouples were affixed to the observation vessel with polyimide tape and connected to the data logger. Vertical movement of the sample unit was controlled remotely.

## Materials

CL was purchased from FUJIFILM Wako Pure Chemical Corp. (Japan). Dicyclohexylmethane 4,4'-diisocyanate (DCMI) mixed isomers and a 60% sodium hydride (NaH) dispersion in liquid paraffin were purchased from Tokyo Chemical Industry Co., Ltd (Japan).

## Sample preparation

To prepare solution A, CL (10.14 g) was first dried at 120 °C for 10 min under reduced pressure. Next, NaH (61.8 mg) was added to the CL under nitrogen at 100 °C, and the mixture was stirred until hydrogen gas generation stopped (~10 min). To prepare solution B, CL (10.10 g) was first dried at 120 °C for 10 min under reduced pressure. DCMI (360  $\mu$ L) was then added under nitrogen at 130 °C. The mixture was stirred for 10 min and allowed to cool to 100 °C.

Solution A, solution B, glass vials and the observation vessel were heated at 100 °C in a globe box under nitrogen. Solution A (450  $\mu$ L) and solution B (450  $\mu$ L) were mixed in a vial at 100 °C, and 430  $\mu$ L of the mixture was immediately injected into the observation vessel. The observation vessel was sealed with screws with seal washers and quickly cooled to room temperature on a quenching block. The observation vessel containing the reaction mixture was kept in a vacuum desiccator prior to measurement.

## Simultaneous measurement conditions

WAXS, temperature measurements, and image collection were performed simultaneously on the BL33XU beam line at the SPring-8 facility. The X-ray energy was 15 keV ( $\lambda = 0.826$  Å), and the detector was situated 181 mm from the observation vessel. 2D photon counting was performed with a PILATUS3 300 K detector (Dectris, Switzerland). The scattering vector ( $q$ ) equaled  $[4\pi \sin(2\theta/2)] \lambda^{-1}$ , where  $2\theta$  is the scattering angle. The accessible  $q$  range spanned from 0.2 Å<sup>-1</sup> to 4.1 Å<sup>-1</sup>. WAXS data were collected once per second, and the temperature was measured every 0.1 s. Images were acquired at 30 frames/s with the web camera. Simultaneous data collection was performed for 10 min after the sample unit started moving. The heating unit was

preheated and held at the selected experimental temperature (120–190 °C) for the measurements.

## Determination of crystallinity

The observation vessel was removed from the heating unit after in situ WAXS analysis and allowed to cool to room temperature. Additional WAXS analysis was then performed at room temperature to determine the crystallinity of PA6. Peaks of the crystalline and amorphous phases were identified in each WAXS spectrum, and the relative crystallinity was calculated as the ratio of the crystalline peak area to the sum of the crystalline and amorphous peak areas.

## Results and discussion

### Visual monitoring and temperature profiles

Typical visual observations and the temperature profile of a vessel set to 150 °C are shown in Fig. 2. Observation was initiated at 26 s for each set of measurements. CL was initially a white solid that melted to form a clear solution. The solution quickly became opaque (~112 s) and yielded a white solid.

The surface temperatures of the observation vessel and the cover glass were monitored, and their profiles during the reaction at 150 °C are shown in Fig. 2. The vessel temperature increased after the vessel was placed in the heating unit. The cover glass temperature increased more slowly than that of the vessel because CL melting was not instantaneous. The cover glass temperature increased at a faster rate after reaching a flexion point, which indicated that CL had completely melted, and then exceeded the 150 °C vessel setting. This was attributed to the exothermic polymerization reaction and crystallization. The temperature peaked at 154 °C, decreased to 148 °C, and remained there for the duration of the measurement. In all subsequent experiments, the average vessel temperature after reaching its peak was recorded as the experimental temperature.

### In situ WAXS analysis

Changes in the WAXS spectrum over time at an experimental temperature of 148 °C are illustrated in Fig. 3. The first WAXS signal for each experiment was recorded at 26 s, which was denoted by  $t_0$ . The crystalline nature of CL disappeared at  $t_m$ , and complete CL melting was accompanied by a shift in the broad halo at 1.0–1.4 Å<sup>-1</sup> ( $q$ ) to a higher angle. This shift indicated a decrease in the distance between molecules as CL began to polymerize. The peak top shift was calculated by fitting each spectrum with the Lorenz function; we defined the polymerization start time  $t_p$

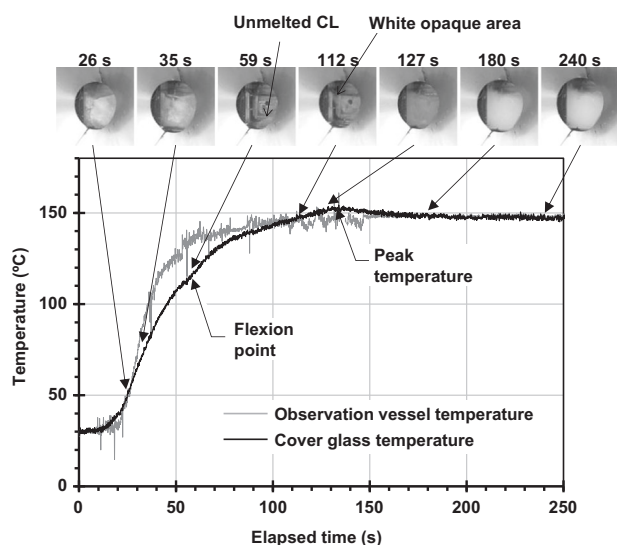


**Fig. 2** Photographic sequence and temperature profile of the reaction at a vessel temperature of 150 °C

as the starting time to shift to a higher angle (refer to Supplementary information). The duration of the transition from  $t_m$  to  $t_p$  was defined as the polymerization induction time, which lasted for 29 s at 148 °C. Following the halo shift, the profile of crystalline PA6 emerged. The starting time to increase the intensity of the main peak was defined as the crystallization starting time,  $t_c$  (refer to Supplementary information). The transition from  $t_p$  to  $t_c$  took 38 s at 148 °C.

We then compared the times shown in Figs. 2 and 3. The CL melting completion time ( $t_m$ ) recorded during visual observation was in agreement with the  $t_m$  determined through temperature measurements and WAXS analysis. The polymerization and crystallization start times were revealed only through WAXS analysis. For this reason, the WAXS results will be the focus of the remaining discussion, and our visual observations and temperature measurements will be considered supporting evidence.

### Temperature dependence

We compared the obtained  $t_m$ ,  $t_p$ , and  $t_c$  values to identify the polymerization and crystallization processes at each experimental temperature. The values of  $t_m$  and  $t_p$  determined with WAXS at experimental temperatures from 120 to ~180 °C are plotted in Fig. 4a, b, respectively. The  $t_c$  values determined via WAXS analysis and by visual inspection are compared in Fig. 4c. The time required to reach complete CL melting ( $t_m$ ) and the onset of polymerization ( $t_p$ ) was reduced as the temperature was increased (Fig. 4a, b). The earliest onset of crystallization occurred at 148 °C. At 166 °C, WAXS analysis revealed that  $t_c$  was higher and increased steadily as the reaction

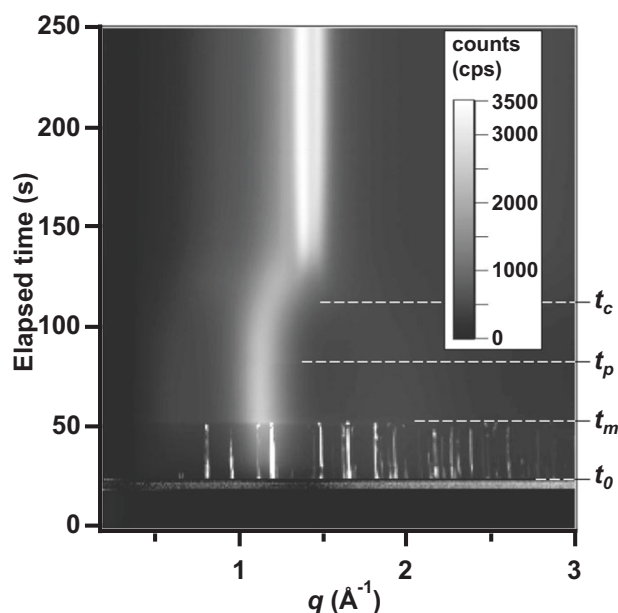


**Fig. 3** WAXS spectrum collected at 150 °C. The CL melting, polymerization, and crystallization temperatures are denoted by  $t_m$ ,  $t_p$ , and  $t_c$ , respectively. WAXS observation began at  $t_0$

temperature was increased. These values are indicated by the open circles in Fig. 4c. The open triangles in Fig. 4c show the times at which the clear CL solutions were visually observed to become opaque. The recorded opacity times and  $t_c$  values determined by WAXS had a similar dependence on the reaction temperature. A comparison of  $t_c$  values and the visually observed opacity start times indicated that crystallization commenced earliest at a reaction temperature of ~150 °C.

We then compared the crystal growth times determined at the various experimental temperatures. We defined  $t_e$  as the point of intersection between the lines tangent to the inflection point (i) and the last 100 intensity measurements (ii) (Fig. 5a). The changes in peak intensities at 166–182 °C showed a rapid increase between 60 and 90 s, which was induced by the shift of the broad halo (refer to Supplementary information). The  $t_e$  values at 166–182 °C were estimated by the increase in intensity after 100 s. The crystallization end time at each experimental temperature is plotted in Fig. 5b. Variations in  $t_e$  with experimental temperature (Fig. 5b) were consistent with changes in WAXS signal intensity over time. The results obtained at 119, 173 and 182 °C are not shown because crystallization was incomplete 10 min after starting the reaction.

### Molding polymerization and crystallization rates

MCPA6 molding was initiated by injecting CL and terminated when the product was removed from the heater. The initiation and completion of the molding process were

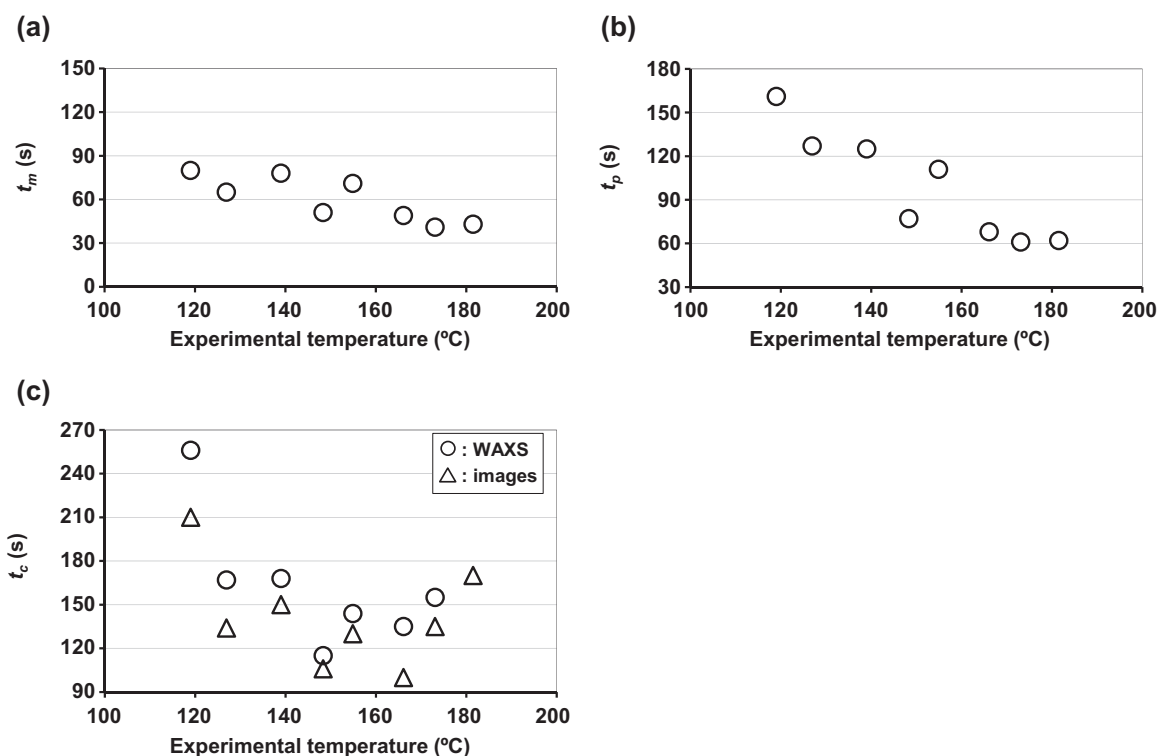


**Fig. 4** Dependence of CL melting, polymerization, and crystallization on reaction temperature. **a**  $t_m$  vs. experimental temperature. **b**  $t_p$  vs. experimental temperature. **c**  $t_c$  determined with WAXS and visually observed opacity time vs. experimental temperature

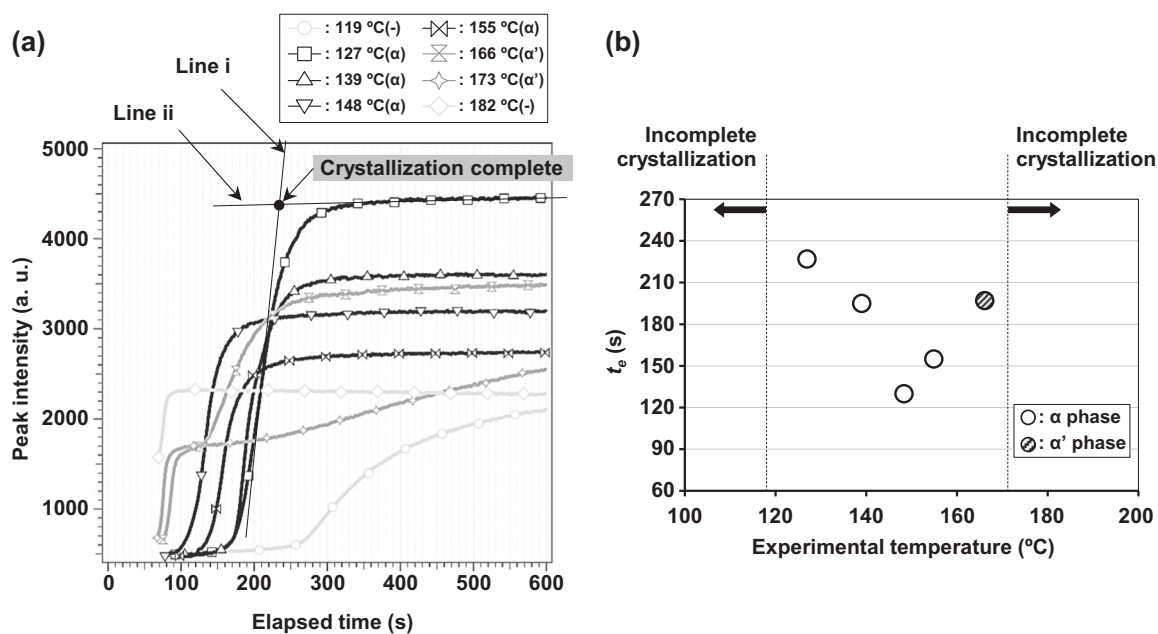


**Fig. 5** WAXS signal intensity over time and  $t_e$  dependence on experimental temperature. **a** Changes in WAXS crystalline signal intensity over time. In the temperature range of 119–155 °C, signals

from 1.61 to 1.68  $\text{\AA}^{-1}$  were assigned to the  $\alpha$  phase of PA6. At 166–182 °C, signals from 1.52 to 1.53  $\text{\AA}^{-1}$  were assigned to the  $\alpha'$  phase of PA6. **b**  $t_e$  at each experimental temperature

defined as  $t_m$  and  $t_e$ , respectively. The calculated molding times based on the in situ WAXS data are plotted in Fig. 6. The molding times at 148 and 155 °C were shorter than

those at other experimental temperatures. The molding process could be divided into the following three phases: polymerization induction ( $t_p - t_m$ ), polymerization ( $t_c - t_p$ )

and crystallization ( $t_e - t_c$ ). The polymerization induction stage became shorter as the temperature increased, and the polymerization stage was shortest at temperatures between 127 and 155 °C. The crystallization stage was shortest at temperatures between 148 and 155 °C. We concluded that shortening the crystallization stage would most effectively reduce the MCPA6 molding time.

### Temperature dependence of PA6 crystallization

The final WAXS spectrum collected at each experimental temperature is shown in Fig. 7a. The WAXS spectra collected after the mixtures cooled to room temperature are shown in Fig. 7b. The  $\alpha$  phase of PA6 was associated with

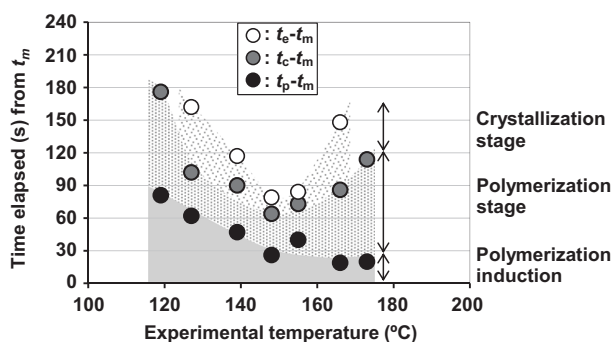


Fig. 6 Total molding times estimated from the WAXS spectra

temperatures from 119–155 °C. The  $\alpha'$  phase of PA6 was observed from 166 to 173 °C, and an amorphous phase was assumed at 182 °C [11]. Each mixture contained the  $\alpha$  phase of PA6 after cooling. These results indicated that the  $\alpha$  crystal phase became predominant during the cooling process.

### Dependence of relative PA6 crystallinity on temperature

We calculated the relative crystallinity of PA6 in each cooled sample by dividing the area of the  $\alpha$ -phase peak by the sum of the crystalline and amorphous peak areas in the WAXS spectrum. The results (Fig. 8) indicated that crystallinity decreased with increasing temperature.

### Reducing MCPA6 molding time

To discuss the molding time of MCPA6, we molded other MCPA6s in a stainless mold on a hot plate and determined their molding time and molecular weight. The molding time of MCPA6 was measured by dielectric analysis (LTF-631, Lambient Technologies). The relationship between the resistivity and the dynamic viscosity was described in the supplementary information. The results are shown in Fig. 9. The surface temperatures of the stainless mold were  $\sim 5$  °C lower than the setting temperature of the hot plate; thus, we

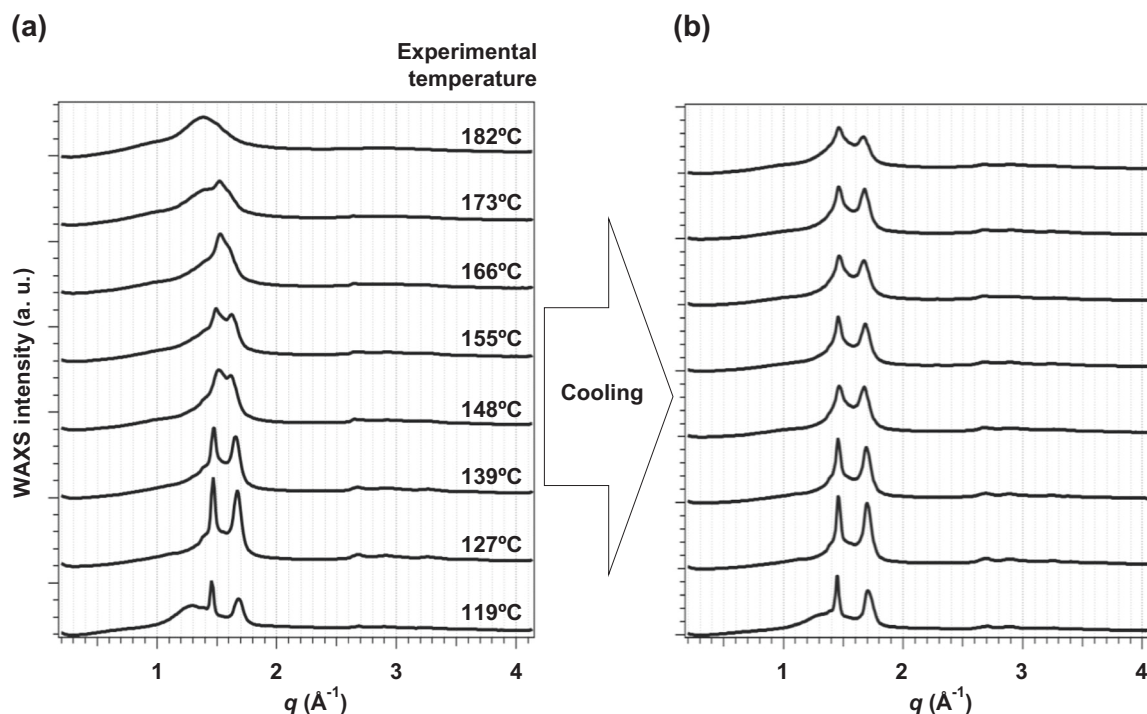
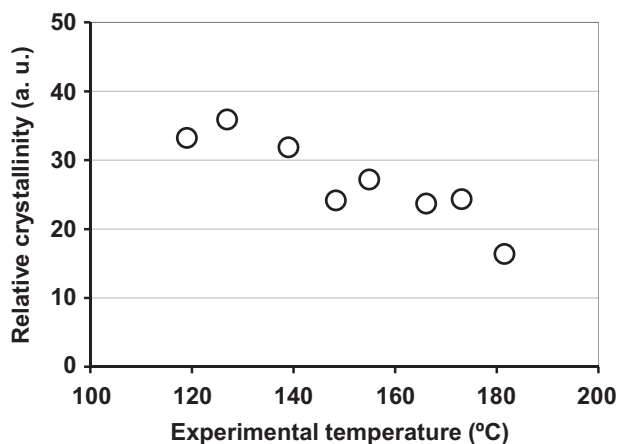
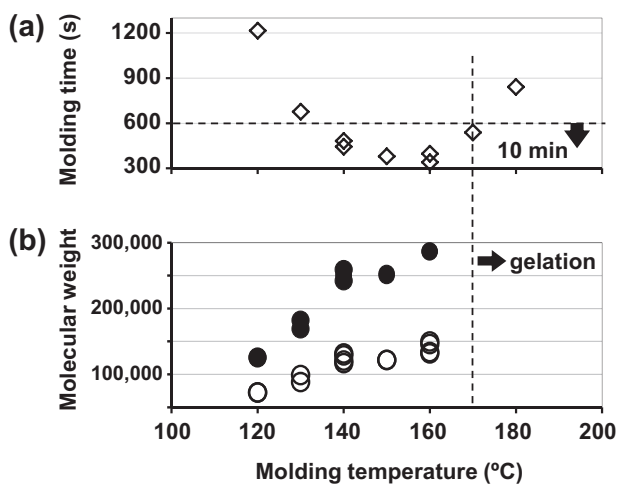


Fig. 7 WAXS spectra of the reaction mixtures. **a** Final in situ WAXS measurements at the experimental temperature. **b** In situ WAXS measurements after cooling to room temperature



**Fig. 8** Relative crystallinity calculated with in situ WAXS data collected at room temperature



**Fig. 9** Experimental MCPA6 molding results. **a** Molding time. **b** PA6 molecular weight (MW). Solid circles: weight-average MW; open circles: number-average MW

considered the setting temperature to be the molding temperature to distinguish it from those used in the WAXS experiments. As shown in Fig. 9a, a curing time of 10 min was too short to complete the polymerization of MCPA6 at molding temperatures of 120, 130 and 180 °C. The molecular weight increased with increasing temperature, and MCPA6 was gelled at temperatures over 170 °C (Fig. 9b). On the basis of the above results, the molding conditions were divided into the following three temperature ranges: <127, >166 °C, and between 139 and 155 °C. The molding times were long at experimental temperatures below 127 °C because the polymerization induction, polymerization and crystallization stages were longer than they were at higher temperatures. This meant that CL was still present after WAXS analysis, and CL acted as a plasticizer during crystallization. In addition, the molecular weight (MW) was lower than it was at experimental temperatures above 140 °C

(Fig. 9b). This resulted in high MCPA6 crystallinity below 127 °C. At experimental temperatures above 166 °C, the polymerization induction stage was short, but the polymerization and crystallization times were long. Lower PA6 crystallinity resulted from the transformation of the  $\alpha'$  phase or the amorphous phase to the  $\alpha$  phase during the cooling process, and gelation occurred at a relatively high molding temperature. The polymerization induction stage at temperatures between 139 and 155 °C was of moderate duration, and the polymerization and crystallization times were short. The polymerization times were nearly equal at these temperatures, but crystallization was especially rapid at 148 and 155 °C (Fig. 6). Magill obtained a maximum PA6 crystallization rate at 138 °C [12]. Our results were not in agreement with those of Magill because our process included CL polymerization and PA6 crystallization. The polymerization induction stage was shortened by increasing the temperature, which meant that the initiation of polymerization and the polymerization rate increased with increasing experimental temperature. This accelerated the formation of PA6 crystal nuclei, and thus, the crystallization rate also increased with increasing temperature. On the other hand, the molecular weight increased with increasing temperature (Fig. 9), which reduced PA6 crystallinity at experimental temperatures between 139 and 155 °C.

## Conclusions

We studied the relationship between the polymerization and crystallization of PA6 via anionic polymerization by performing in situ WAXS analysis, temperature measurements and visual observations simultaneously. In situ WAXS enabled discrimination between the polymerization of  $\epsilon$ -caprolactam and the crystallization of PA6. We compared the polymerization rates, crystallization rates and crystallinity determined with the WAXS data. The polymerization rate was higher at elevated temperatures, while the crystallization rate was highest at temperatures between 148 and 155 °C. Consequently, the total molding time from CL melting to complete PA6 crystallization was shortest at 148 and 155 °C. The crystallinity decreased as the experimental temperature increased because the MW of PA6 increased with increasing temperature. We concluded that a molding temperature between 148 and 155 °C was most suitable for producing MCPA6 with the desired properties.

**Acknowledgements** The authors would like to thank Mr Chisao Hayashi and Mr Masao Tsuji at the Toyota Central R&D Labs and Prof. Kenzo Fukumori at the Aichi Institute of Technology for their valuable input. The synchrotron radiation experiments were performed on the BL33XU line at SPring-8 with the approval of the Japan Synchrotron Radiation Research Institute (JASRI) (Proposal Nos. 2016A7003 and 2016B7003).

## Compliance with ethical standards

**Conflict of interest** The authors declare that they have no conflict of interest.

**Publisher's note** Springer Nature remains neutral with regard to jurisdictional claims in published maps and institutional affiliations.

## References

1. Roda J. Polyamides. In: Dubois P, Coulembier O, Raquez JM, editors. Handbook of ring-opening polymerization. Weinheim: Wiley-VCH Verlag; 2009, p. 165–81.
2. Bitterlich M. Tailored to reactive polyamide 6. *Kunstst Int*. 2014;3:47–51. <https://www.kunststoffe.de/en/journal/archive/article/tailored-to-reactive-polyamide-6-814047.html>. Accessed 17 Apr 2019.
3. Wilfong DL, Pommerening CA, Gardlund ZG. Separation of polymerization and crystallization processes for nylon-6. *Polymer*. 1992;33:3884–8.
4. Khodabakhshi K, Gilbert M, Dickens P. Monitoring of small scale anionic polymerization of caprolactam: a method to be used in an additive manufacturing process. *Polym Adv Technol*. 2013;24:503–10.
5. Sibal PW, Camargo RE, Macosko CW. Designing nylon-6 polymerization systems for RIM. *Polym Process Eng*. 1983;1:147–69.
6. Davé RS, Kruse RL, Stebbins LR, Udipi K. Polyamides from lactams via anionic ring-opening polymerization: 2. kinetics. *Polymer*. 1997;38:939–47.
7. Ramesh C, Gowd EB. High-temperature X-ray diffraction studies on the crystalline transitions in the  $\alpha$ - and  $\gamma$ -forms of nylon-6. *Macromolecules*. 2001;34:3308–13.
8. Van Rijswij K, Bersee HEN, Jager WF, Picken SJ. Optimisation of anionic polyamide-6 for vacuum infusion of thermoplastic composites: choice of activator and initiator. *Compos, Part A*. 2006;37:949–56.
9. Van Rijswij K, Bersee HEN, Beukers A, Picken SJ, Van Geenen AA. Optimisation of anionic polyamide-6 for vacuum infusion of thermoplastic composites: influence of polymerisation temperature on matrix properties. *Polym Test*. 2006;25:392–404.
10. Ricco L, Russo S, Orefice G, Riva F. Anionic poly( $\epsilon$ -caprolactam): relationships among conditions of synthesis, chain regularity, reticular order, and polymorphism. *Macromolecules*. 1999;32:7726–31.
11. Murthy NS, Curran SA, Aharoni SM, Minor H. Premelting crystalline relaxations and phase transitions in nylon 6 and 6,6. *Macromolecules*. 1991;24:3215–20.
12. Magill JH. Crystallization kinetics study of nylon 6. *Polymer*. 1962;3:655–64.